Int. J. Solids Structures Vol. 29, No. 5, pp. 641-652, 1992
Printed in Great Britain.

0020-7683/92 $5.00+.00

INFLUENCE OF INERTIA AND DISSIPATIVE FORCES ON THE DYNAMIC RESPONSE OF POROELASTIC MATERIALS

HUOY-SHYI TSAY
Chung Shan Institute of Science and Technology, P.O. Box 90008-9-2, Lung-Tan, Taiwan 32526, R.O.C.

and

HERBERT B. KINGSBURY
Department of Mechanical Engineering, University of Delaware, Newark, DE 19716 U.S.A.

(*Received* 4 *October* 1990; *in revised form* 4 *June* 1991)

Abstract—This paper derives a complex dynamic stiffness function for a poroelastic layer and uses this to examine the range of validity of solutions to Biot's dynamic poroelasticity equations when either inertia or dissipation terms are neglected. It also examines the effects of certain inertia terms and of surface boundary conditions on the solutions to these equations and presents a systematic study of the effect of the dissipation term of Biot's theory on the system storage and loss moduli.

Biot's equations of poroelasticity are first phrased in terms of a single equation which governs both the fluid and solid phase dilatational strains. A general solution to these equations is derived in the Laplace domain and expressions for the displacement and stress Laplace transforms in a poroelastic layer are obtained. The constants of integration occurring in these solutions are next evaluated for the case of an impulsive load applied to one surface of the layer. Cases of both a permeable and an impermeable loaded surface are considered. The resulting solutions for the Laplace transform of the impulsive excitation response are then transformed into frequency domain complex response functions, called dynamic stiffness functions, which characterize the stiffness and damping of the layer. Parametric studies are then carried out employing these complex frequency response functions.

INTRODUCTION

Poroelastic materials are materials consisting of fluid-filled porous elastic solids. When the material is deformed, the volume which contains the fluid is changed. Both the dynamic stiffness of the material and the energy loss associated with its deformation are affected by the flow of the viscous fluid within it. The mechanism of the energy dissipation of a poroelastic material differs from that of a conventional solid material because of the interactions between the fluid and the solid.

In a series of papers, Biot (1941, 1955, 1956a, b) and Biot and Willis (1957) introduced a general theory of linear poroelasticity. A number of investigators have used Biot's theory to study consolidation problems or the response of poroelastic materials to uniformly moving or harmonically time varying loads. Although mathematical difficulties in solving the complete equations have usually prompted neglect of either inertia terms or dissipation terms, Biot's complete dynamic equations have been used to study one-dimensional wave propagation in semi-infinite poroelastic media by Biot (1956b), Chakravarti (1962), Garg *et al.* (1974) and Hong *et al.* (1988) among others.

Wijesinghe and Kingsbury (1979) and Kingsbury (1984) used Biot's equations to examine the complex modulus, which is a measure of dynamic stiffness, of a poroelastic slab with a permeable upper surface. They investigated both the "quasi-static" case without inertia terms and the "dynamic" (reduced dynamic) case without dissipation terms, thereby allowing coupling terms involving either the dissipation or the inertia forces of the governing equations to be neglected. Harmonic excitation was applied to the upper surface of the poroelastic slab and the complex modulus for the poroelastic slab then determined. Subsequently Okuno and Kingsbury (1989) extended the previous work to study energy dissipation and complex moduli in problems involving two dimensional tension compression and bending deformation of poroelastic materials; again by determining response to harmonic excitation using Biot's quasi-static equations.

The present paper studies the effects of inertia and dissipation coupling in Biot's complete equations by comparing the calculated response of a poroelastic layer based on the complete governing equation with previously calculated response obtained on the basis of equations which neglect either inertia or dissipation terms. It also uses the derived solutions to examine the effects of the dissipation coefficient, the mass coupling parameter and surface flow effects on the predicted response of a poroelastic structure.

The response of the layer is first characterized in the Laplace domain by means of a dynamic stiffness transfer function $[K(s)]$ which is defined as the ratio of the Laplace Transform of the force excitation $[I(s)]$ to that of the displacement response $[O(s)]$. $K(s)$ is obtained by evaluating the constants of integration arising from the solution to Biot's full dynamic equations for the case of a slab with fixed lower surface and upper surface subjected to an impulse loading.

Once the transfer function of the system is known, a frequency response function, called the "complex dynamic stiffness" which characterizes the steady state response in the frequency domain, can be easily obtained by replacing the Laplace transform parameter s by $i\omega$ where ω is the frequency parameter.

The complex modulus, as derived by Wijesinghe and Kingsbury (1979), is a material property which describes both the stiffness and damping in a material and can be obtained from the complex dynamic stiffness at frequencies below the first natural frequency of the structure.

Numerical results for the dimensionless complex dynamic stiffness for a poroelastic slab with permeable and impermeable surfaces, are illustrated and discussed. Comparisons of the results obtained from the present study with the results of the earlier study by Wijesinghe and Kingsbury (1979) for a poroelastic slab with a permeable upper surface are then made. Finally, the effects of the dissipation coefficient, b, and the coupling mass density, ρ_{12}, on this dimensionless complex dynamic stiffness function are investigated.

THE GOVERNING EQUATIONS

Biot's theory of linear, isotropic poroelasticity is employed in this study. This formulation assumes the porous material is constructed such that a solid material forms a structure which contains statistically distributed small pores that are filled with a Newtonian-viscous compressible fluid. The bulk material is assumed to be homogeneous on a macroscopic scale, and the pores are assumed to be interconnected. The solid skeleton is taken to be linear elastic and undergoing small deformation. The fluid flow is assumed to be of the Poiseuille type so that the fluid inertia and the friction are uniquely characterized by the density, viscosity and the pore dimensions.

The equations governing the deformation of poroelastic materials given by Biot (1956b) can be written as

$$N\nabla^2\mathbf{u}+\text{grad}\,[(A+N)e+Q\varepsilon] = \frac{\partial^2}{\partial t^2}(\rho_{11}\mathbf{u}+\rho_{12}\mathbf{U})+b\frac{\partial}{\partial t}(\mathbf{u}-\mathbf{U}), \tag{1}$$

$$\text{grad}\,[Qe+R\varepsilon] = \frac{\partial^2}{\partial t^2}(\rho_{12}\mathbf{u}+\rho_{22}\mathbf{U})-b\frac{\partial}{\partial t}(\mathbf{u}-\mathbf{U}), \tag{2}$$

where N, A, Q and R are material constants and the dissipation coefficient b is defined as $b=\mu\phi^2/\kappa$ in which μ is the fluid viscosity, ϕ is the porosity, κ is Darcy's coefficient of intrinsic permeability, $\mathbf{u}$ is the average solid displacement vector, and $\mathbf{U}$ is the average fluid displacement. The solid dilatation, e, and the fluid dilatation, ε, are defined in the usual manner for small deformation. The quantities ρ_{11}, ρ_{12} and ρ_{22} are apparent mass densities, which take into account the non-uniformity of the relative fluid flow through the pores. When there is no relative motion between the fluid and the solid, ρ, the total mass density of the fluid-saturated material is given by: $\rho=\rho_{11}+\rho_{22}+2\rho_{12}$. ρ can be expressed in terms of the mass density of solid, ρ_s, and the mass density of fluid, ρ_f, as $\rho=(1-\phi)\rho_s+\phi\rho_f=\rho_1+\rho_2$ in which ρ_1 and ρ_2 are the mass densities per unit total volume of the solid

and fluid, respectively. Biot showed that $\rho_1 = \rho_{11} + \rho_{12}$ and $\rho_2 = \rho_{12} + \rho_{22}$. It is noted that ρ_{11} represents the total effective mass of the solid moving in the fluid, ρ_{22} represents the total effective mass of that part of the fluid, and ρ_{12} represents a mass coupling parameter between the fluid and the solid and these coefficients cannot be uniquely determined in terms of the fluid and solid phase densities. Biot (1956b) also shows that the mass coefficients have the following properties:

$$\rho_{11} \geqslant 0, \quad \rho_{22} \geqslant 0, \quad \rho_{12} \leqslant 0.$$

The dynamic equilibrium equations of a poroelastic element in terms of skeleton and fluid dilatational strains for poroelastic materials can be obtained by taking the divergence of eqns (1) and (2) which yields

$$\nabla^2(Pe+Qe) = \frac{\partial^2}{\partial t^2}(\rho_{11}e+\rho_{12}\varepsilon)+b\frac{\partial}{\partial t}(e-\varepsilon), \tag{3}$$

$$\nabla^2(Qe+Re) = \frac{\partial^2}{\partial t^2}(\rho_{12}e+\rho_{22}\varepsilon)-b\frac{\partial}{\partial t}(e-\varepsilon), \tag{4}$$

where $P = 2N+A$. After rearrangements, eqns (3) and (4) can be written in the following forms:

$$\left(P\nabla^2-\rho_{11}\frac{\partial^2}{\partial t^2}-b\frac{\partial}{\partial t}\right)e = \left(-Q\nabla^2+\rho_{12}\frac{\partial^2}{\partial t^2}-b\frac{\partial}{\partial t}\right)\varepsilon, \tag{5}$$

$$\left(Q\nabla^2-\rho_{12}\frac{\partial^2}{\partial t^2}+b\frac{\partial}{\partial t}\right)e = \left(-R\nabla^2+\rho_{22}\frac{\partial^2}{\partial t^2}+b\frac{\partial}{\partial t}\right)\varepsilon. \tag{6}$$

Substituting the ε in eqn (6) in terms of e into eqn (5), yields

$$\left[\beta_1\nabla^4-\left(\beta_2\frac{\partial}{\partial t}+\alpha_1\frac{\partial^2}{\partial t^2}\right)\nabla^2+\left(\rho_0\frac{\partial}{\partial t}+b\rho\right)\frac{\partial^3}{\partial t^3}\right]e = 0, \tag{7}$$

where

$$\begin{aligned}
\beta_1 &= PR-Q^2,\\
\beta_2 &= (P+R+2Q)b,\\
\alpha_1 &= P\rho_{22}+R\rho_{11}-2Q\rho_{12},\\
\rho_0 &= \rho_{11}\rho_{22}-\rho_{12}^2,\\
\rho &= \rho_{11}+\rho_{22}+2\rho_{12}.
\end{aligned}$$

Similarly, the elimination of e in eqns (5) and (6) yields the same differential equation for ε. It is noted that eqn (7) has been derived by Chakravarti (1962) for obtaining the dynamic stress in a poroelastic infinite medium with a spherical cavity.

In this study, the systems considered are assumed to be deformed from the initially undeformed position and all stresses are zero at $t = 0$.

INTEGRAL TRANSFORM SOLUTIONS

By taking the Laplace Transform of the differential equations of solid and fluid dilatational strains, eqn (7), and using the initial conditions, bi-harmonic equations for the solid and the fluid dilatational strains in the transform domain can be derived. Since the differential equations for both dilatational strains are the same, the form of the general

solutions for both are the same except for integration constants. Taking the Laplace Transform with respect to time of eqns (6) and (7) and using the initial conditions, yields

$$(Q\nabla^2 - \rho_{12}s^2 + bs)\bar{e} = (-R\nabla^2 + \rho_{22}s^2 + bs)\bar{\varepsilon}, \tag{8}$$

$$\left(\nabla^4 - \frac{\beta_2 s + \alpha_1 s^2}{\beta_1}\nabla^2 + \frac{\rho_0 s + \rho b}{\beta_1}s^3\right)\bar{e} = 0, \tag{9}$$

where $\bar{e}$ and $\bar{\varepsilon}$ are the Laplace Transforms of e and ε. Equation (9) can be rewritten as a product of two modified Helmholtz equations:

$$(\nabla^2 - \delta_1^2)(\nabla^2 - \delta_2^2)\bar{e} = 0, \tag{10}$$

where

$$\delta_1 = \pm\sqrt{\frac{s\Psi_2}{2\beta_1}}, \quad \delta_2 = \pm\sqrt{2}s\sqrt{\frac{\Psi_4}{\Psi_2}}$$

and

$$\Psi_1 = (\alpha_1 s + \beta_2)^2 - 4\beta_1 s(\rho_0 s + b\rho),$$
$$\Psi_2 = \sqrt{\Psi_1} + \alpha_1 s + \beta_2,$$
$$\Psi_4 = \rho_0 s + b\rho.$$

The solution for one-dimensional flow and deformation in a layer with transverse co-ordinate z and thickness h is next obtained.

The skeleton dilatational strain $\bar{e}$ can be found by superposition of the solutions obtained for each of the operators in eqn (10) in the form ($\bar{e} = \bar{e}_1 + \bar{e}_2$) with the solutions for $\bar{e}_1$ and $\bar{e}_2$ obtained from

$$(\nabla^2 - \delta_1^2)\bar{e}_1 = 0, \tag{11}$$

$$(\nabla^2 - \delta_2^2)\bar{e}_2 = 0. \tag{12}$$

In one-dimensional Cartesian co-ordinates, $\nabla^2 = \partial^2/\partial z^2$, and the solutions to eqns (11) and (12) are combined to yield

$$\bar{e} = A_1 \exp(\delta_1 z) + A_2 \exp(-\delta_1 z) + A_3 \exp(\delta_2 z) + A_4 \exp(-\delta_2 z). \tag{13}$$

The same procedure yields the fluid dilatation:

$$\bar{\varepsilon} = B_1 \exp(\delta_1 z) + B_2 \exp(-\delta_1 z) + B_3 \exp(\delta_2 z) + B_4 \exp(-\delta_2 z). \tag{14}$$

A_i and B_i ($i = 1, 2, 3, 4$) appearing in eqns (13) and (14) are constants.

The relationship between the coefficients A_i and B_i can be found by substituting $\bar{e}$, eqn (13), and $\bar{\varepsilon}$, eqn (14), into eqn (8) which yields

$$B_i = C_i A_i \quad (i = 1, 2, 3, 4),$$

where

$$C_1 = C_2 = \frac{-\rho_{12}s^2 + bs + Q\delta_1^2}{\rho_{22}s^2 + bs - R\delta_1^2}, \tag{15}$$

$$C_3 = C_4 = \frac{-\rho_{12}s^2 + bs + Q\delta_2^2}{\rho_{22}s^2 + bs - R\delta_2^2}. \tag{16}$$

The expressions for the dilatational strains $\bar{e}$ and $\bar{\varepsilon}$ are substituted in the Laplace transformed forms of eqns (1) and (2) to obtain the expressions for skeleton and fluid displacements (**u** and **U**).

The solid phase displacement $\bar{\mathbf{u}}(s)$ becomes

$$\bar{\mathbf{u}}(s) = \frac{\begin{vmatrix} P\dfrac{d\bar{e}}{dz} + Q\dfrac{d\bar{\varepsilon}}{dz} & \rho_{12}s^2 - bs \\ Q\dfrac{d\bar{e}}{dz} + R\dfrac{d\bar{\varepsilon}}{dz} & \rho_{22}s^2 + bs \end{vmatrix}}{\begin{vmatrix} \rho_{11}s^2 + bs & \rho_{12}s^2 - bs \\ \rho_{12}s^2 - bs & \rho_{22}s^2 + bs \end{vmatrix}}$$

$$= \frac{\Delta_1}{\Delta}\frac{d\bar{e}}{dz} + \frac{\Delta_2}{\Delta}\frac{d\bar{\varepsilon}}{dz}, \tag{17}$$

where

$$\Delta = (\rho_0 s + b\rho)s^2,$$
$$\Delta_1 = (\rho_{22}s + b)P - (\rho_{12}s - b)Q,$$
$$\Delta_2 = (\rho_{22}s + b)Q - (\rho_{12}s - b)R.$$

The following result for $\bar{\mathbf{u}}(s)$ is obtained by substituting the results for $\bar{e}$, eqn (13), and $\bar{\varepsilon}$, eqn (14), into eqn (17).

$$\bar{\mathbf{u}}(s) = \left(\frac{\Delta_1}{\Delta} + \frac{\Delta_2 C_1}{\Delta}\right)\delta_1[A_1 \exp(\delta_1 z) - A_2 \exp(-\delta_1 z)]$$
$$+ \left(\frac{\Delta_1}{\Delta} + \frac{\Delta_2 C_3}{\Delta}\right)\delta_2[A_3 \exp(\delta_2 z) - A_4 \exp(-\delta_2 z)]. \tag{18}$$

Next, using the stress definitions and stress-strain relationships of Biot and Willis (1957) and the results of solid and fluid strains, the solid stress, $\bar{\sigma}_{zz}$, and the fluid stress, $\bar{\sigma}$, for the one-dimensional problems become

$$\bar{\sigma}_{zz}(s) = 2N\frac{\partial\bar{\mathbf{u}}}{\partial z} + A\bar{e} + Q\bar{\varepsilon} = P\bar{e} + Q\bar{\varepsilon} = (P + QC_1)[A_1 \exp(\delta_1 z) + A_2 \exp(-\delta_1 z)]$$
$$+ (P + QC_3)[A_3 \exp(\delta_2 z) + A_4 \exp(-\delta_2 z)], \tag{19}$$

$$\bar{\sigma}(s) = Q\bar{e} + R\bar{\varepsilon} = (Q + RC_1)[A_1 \exp(\delta_1 z) + A_2 \exp(-\delta_1 z)]$$
$$+ (Q + RC_3)[A_3 \exp(\delta_1 z) + A_4 \exp(-\delta_1 z)]. \tag{20}$$

DYNAMIC STIFFNESS TRANSFER FUNCTIONS

Next, the Laplace transform of the system response to an impulsive excitation is obtained to yield the system transfer function $[\bar{K}(s)]$ which is the ratio of the Laplace Transform of the force excitation, $I(s)$, to that of the displacement response, $O(s)$, under the

assumption that all initial conditions are zero. If an excitation is an impulse, $I(s) = 1$, then the transfer function is exactly the reciprocal of the Laplace Transform of impulsive response.

Once $\bar{K}(s)$ is obtained from impulse analysis, the response to any excitation can, in theory, be determined by formulating $I(s)$ and then finding the inverse Laplace transform of $I(s)\,\bar{K}(s)$. Since $\bar{K}(s)$ is the ratio of force excitation to displacement response, it is denoted as the "dynamic stiffness transfer function".

Using the general solutions for the strain, stress and displacement transforms and applying the suitable boundary conditions, the unknown integration coefficients, A_i $(i = 1, 2, 3, 4)$, appearing in the general solutions for strains and displacements of the solid and the fluid are determined. Transfer functions are then obtained for layers with permeable and impermeable upper surfaces.

AN INFINITE POROELASTIC LAYER WITH A PERMEABLE UPPER SURFACE

In this case, the load applied on the upper surface is represented as $\tau_{zz} = p_0\delta(t)$ where p_0 is the amplitude of the impulsive loading. Here, $\tau_{zz} = \sigma_{zz} + \sigma$ in which σ_{zz}, eqn (19), is the stress acting on the solid portions of the upper surface and σ, eqn (20), is the stress acting on the fluid portions. Since the upper surface is permeable, the fluid pressure, p, $(p = -\sigma/\phi)$ is taken as zero. The lower surface of the poroelastic slab is fixed on a rigid and impermeable plane. Accordingly, the solid displacement $\mathbf{u}$ must be zero and the impermeable boundary condition implies a zero fluid pressure gradient on this face $(\partial p/\partial z = 0)$.

Making use of the stress–strain results, the Laplace transforms of the boundary condition equations become

$$\begin{aligned}
\bar{\sigma}_{zz|z=h} &= 2N\bar{e}_{zz} + A\bar{e} + Q\bar{\varepsilon} = P\bar{e} + Q\bar{\varepsilon} = p_0,\\
\bar{\sigma}_{|z=h} &= Q\bar{e} + R\bar{\varepsilon} = 0,\\
\bar{\mathbf{u}}_{|z=0} &= 0,\\
\frac{\mathrm{d}\bar{\sigma}}{\mathrm{d}z}_{|z=0} &= Q\frac{\mathrm{d}\bar{e}}{\mathrm{d}z} + R\frac{\mathrm{d}\bar{\varepsilon}}{\mathrm{d}z} = 0.
\end{aligned} \tag{21}$$

Substitution of the expressions for $\bar{e}$, eqn (13), $\bar{\varepsilon}$, eqn (14), and $\bar{\mathbf{u}}$ eqn (18), into eqn (21) gives

$$\begin{aligned}
\bar{\sigma}_{zz|z=h} &= (P-QC_1)A_1\exp(\delta_1 h) + (P+QC_1)A_2\exp(-\delta_1 h)\\
&\quad + (P+QC_3)A_3\exp(\delta_2 h) + (P+QC_3)A_4\exp(-\delta_2 h) = p_0,\\
\bar{\sigma}_{|z=h} &= (Q-RC_1)A_1\exp(\delta_1 h) + (Q+RC_1)A_2\exp(-\delta_1 h)\\
&\quad + (Q+RC_3)A_3\exp(\delta_2 h) + (Q+RC_3)A_4\exp(-\delta_2 h) = 0,\\
\bar{\mathbf{u}}_{|z=0} &= \delta_1\left(\frac{\Delta_1}{\Delta} + \frac{\Delta_2 C_1}{\Delta}\right)A_1 - \delta_1\left(\frac{\Delta_1}{\Delta} + \frac{\Delta_2 C_1}{\Delta}\right)A_2\\
&\quad + \delta_2\left(\frac{\Delta_1}{\Delta} + \frac{\Delta_2 C_3}{\Delta}\right)A_3 - \delta_2\left(\frac{\Delta_1}{\Delta} + \frac{\Delta_2 C_3}{\Delta}\right)A_4 = 0,\\
\frac{\mathrm{d}\bar{\sigma}}{\mathrm{d}z}_{|z=0} &= (Q+RC_1)\delta_1 A_1 - (Q+RC_1)\delta_1 A_2 + (Q+RC_3)\delta_2 A_3 - (Q+RC_3)\delta_2 A_4 = 0.
\end{aligned} \tag{22}$$

Upon solving the equation set (22), the following results for the coefficients A_1, A_2, A_3 and A_4 are obtained:

$$A_1 = A_2 = \frac{p_0(C_3R+Q)}{\beta_1(C_3-C_1)[\exp(\delta_1 h)+\exp(-\delta_1 h)]},$$

$$A_3 = A_4 = \frac{p_0(C_1R+Q)}{\beta_1(C_1-C_3)[\exp(\delta_2 h)+\exp(-\delta_2 h)]}. \tag{23}$$

With the substitution of eqn (23) into eqn (18), the final result for the solid displacement transform, $\bar{\mathbf{u}}(s)$ becomes

$$\bar{\mathbf{u}}(s) = p_0\left[\frac{\delta_1(C_3R+Q)}{\beta_1(C_3-C_1)}\frac{\Delta_1+\Delta_2C_1}{\Delta}\frac{\exp(\delta_1 z)-\exp(-\delta_1 z)}{\exp(\delta_1 h)+\exp(-\delta_1 h)}\right.$$
$$\left.+\frac{\delta_2(C_1R+Q)}{\beta_1(C_1-C_3)}\frac{\Delta_1+\Delta_2C_3}{\Delta}\frac{\exp(\delta_2 z)-\exp(-\delta_2 z)}{\exp(\delta_2 h)+\exp(-\delta_2 h)}\right]. \tag{24}$$

Finally, the dynamic stiffness transfer function is obtained as

$$\bar{K}(s) = \frac{p_0}{\bar{\mathbf{u}}(s)_{|z=h}} = [\beta_1(C_3-C_1)]\Big/$$
$$\left[\delta_1\tanh(\delta_1 h)(C_3R+Q)\frac{\Delta_1+\Delta_2C_1}{\Delta}-\delta_2\tanh(\delta_2 h)(C_1R+Q)\frac{\Delta_1+\Delta_2C_3}{\Delta}\right]. \tag{25}$$

AN INFINITE LAYER WITH AN IMPERMEABLE UPPER SURFACE

The boundary conditions for this case in the Laplace Transform domain are given by

$$\bar{\tau}_{zz|z=h} = (P+Q)\bar{e}+(Q+R)\bar{\varepsilon} = p_0,$$
$$\frac{\mathrm{d}\bar{\sigma}}{\mathrm{d}z_{|z=h}} = Q\frac{\mathrm{d}\bar{e}}{\mathrm{d}z}+R\frac{\mathrm{d}\bar{\varepsilon}}{\mathrm{d}z} = 0,$$
$$\bar{\mathbf{u}}_{|z=0} = 0,$$
$$\frac{\mathrm{d}\bar{\sigma}}{\mathrm{d}z_{|z=0}} = Q\frac{\mathrm{d}\bar{e}}{\mathrm{d}z}+R\frac{\mathrm{d}\bar{\varepsilon}}{\mathrm{d}z} = 0. \tag{26}$$

After solving the above equation set and obtaining the coefficient results A_i ($i = 1, 2, 3, 4$), the final result for $\bar{\mathbf{u}}(s)$ at $z = h$ becomes:

$$\bar{\mathbf{u}}(s) = \left\{p_0\delta_1\delta_2\tanh(\delta_1 h)\tanh(\delta_2 h)\left[\frac{\Delta_1+\Delta_2C_1}{\Delta}(Q+RC_3)\right.\right.$$
$$\left.\left.-\frac{\Delta_1+\Delta_2C_3}{\Delta}(Q+RC_1)\right]\right\}\Big/\{\delta_2\tanh(\delta_2 h)(P+Q+RC_1+QC_1)(Q+RC_3)$$
$$-\delta_1\tanh(\delta_1 h)(P+Q+RC_3+QC_3)(Q+RC_1)\}. \tag{27}$$

Using the above displacement result, the transfer function for this case is

$$\bar{K}(s) = \{\delta_2\tanh(\delta_2 h)(P+Q+RC_1+QC_1)(Q+RC_3)$$
$$-\delta_1\tanh(\delta_1 h)(P+Q+RC_3+QC_3)(Q+RC_1)\}\Big/\left\{\delta_1\delta_2\tanh(\delta_1 h)\tanh(\delta_2 h)\right.$$
$$\left.\times\left[\frac{\Delta_1+\Delta_2C_1}{\Delta}(Q+RC_3)-\frac{\Delta_1+\Delta_2C_3}{\Delta}(Q+RC_1)\right]\right\}. \tag{28}$$

Table 1. Material properties of a poroelastic specimen

P^*	5.477784
Q^*	0.708907
R^*	0.275563
b^*	9.300564
ρ_{11}^*	3.701853E-9
ρ_{22}^*	1.133610E-9
ρ_{12}^*	−0.875100E-9

THE COMPLEX DYNAMIC STIFFNESS FUNCTION

If a transfer function of a system is given in the Laplace domain, the frequency domain results can be obtained simply by changing the Laplace Transform parameter to $i\omega$, where ω is a frequency parameter. The dynamic stiffness transfer function $\bar{K}(s)$ is then transformed into a complex function of frequency, $\bar{K}(i\omega)$, which is called the complex dynamic stiffness function.

The complex dynamic stiffness function $\bar{K}(i\omega)$ may be represented in terms of its real and imaginary parts as $\bar{K} = \bar{K}' + i\bar{K}''$ or $\bar{K} = \bar{K}'(1 + i\eta)$ where η is the loss tangent, $\bar{K}''$ is the lost stiffness and $\bar{K}'$ is the dynamic stiffness. $\bar{K}''$ and η are measures of energy dissipation in the system.

Before evaluating the complex dynamic stiffness function in the frequency domain, the parameters appearing in $\bar{K}(i\omega)$ are first non-dimensionalized in the following manner:

$$\bar{u}^* = \frac{\bar{u}}{h}, \quad z^* = \frac{z}{h}, \quad P^* = \frac{P}{N}, \quad Q^* = \frac{Q}{N}, \quad R^* = \frac{R}{N},$$

$$p_0^* = \frac{p_0}{N}, \quad \omega^* = \omega/\omega_0, \quad b^* = \frac{bh^2 s_0}{N}, \quad \rho_{ij}^* = \frac{\rho_{ij} h^2 s_0^2}{N} \quad (i, j = 1, 2),$$

where ω_0 is an arbitrary constant. Since results of this study are to be compared with results presented by Wijesinghe and Kingsbury (1979), poroelastic material properties used by those authors are employed in this study and shown in dimensionless form in Table 1.† These data represent the estimated properties for the compact bone but are otherwise arbitrarily chosen.

EFFECTS OF SURFACE PERMEABILITY

The dimensionless dynamic stiffness, $\bar{K}'$, and the loss tangent, η, of the infinite poroelastic slab with permeable and impermeable surfaces with the properties of Table 1 are shown in Figs 1 and 2, respectively.

For the case of the impermeable upper surface, there is no relative motion between the fluid and solid phases so the entire poroelastic material behaves as an elastic solid. The stiffness remains constant and the loss constant remains zero below the first resonant frequency of the layer. In the case of the permeable surface, on the other hand, the stiffness is less at low frequencies but then increases to reach that of the impermeable surface case at high frequencies. At very low frequencies, the entire stiffness of the slab is provided by the solid phase alone, while at very high frequencies there is little relative motion of the fluid with respect to the solid. It is in the intermediate frequency range that the energy dissipated by the fluid flow relative to the solid skeleton becomes maximum resulting in a maximum in the loss tangent as shown in Fig. 2. The frequency at which the loss tangent is maximum will be denoted as the "critical" frequency, ω_c, in this paper.

† $\lambda^* = 1.49 \times 10^6$ lb in^{-2}, $M = 0.9 \times 10^6$ lb in^{-2}, $R = 0.248 \times 10^6$ lb in^{-2}, $Q = 0.638 \times 10^6$ lb in^{-2}, $A = 3.13 \times 10^6$ lb in^{-2}, $\phi = 0.14$, $b = 2.54 \times 10^6$ lb s in^{-4}, $h = 10^{-1}$ m and $s_0 = 1$ s^{-1} are assumed.

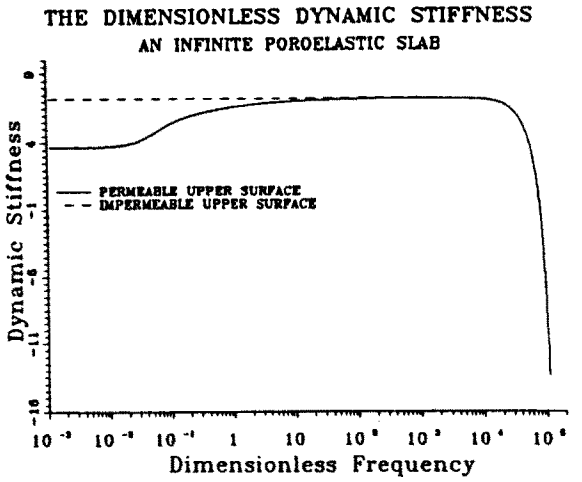

Fig. 1. The dimensionless dynamic stiffness for an infinite poroelastic slab.

COMPARISON OF DYNAMIC RESULTS AND QUASI-STATIC RESULTS

The range of applicability of the quasi-static and dissipationless dynamic theories to poroelastic structural response analysis is next explored. Results for the dimensionless complex dynamic stiffness function obtained from the present study, eqn (24), and the results for complex modulus obtained from Wijesinghe and Kingsbury's quasi-static analysis for an infinite poroelastic slab with a permeable upper surface are compared in Fig. 3. Figure 3 shows that the results of the two are essentially identical in the range of frequencies below the fundamental resonant frequency of the slab. The dimensionless dynamic stiffness $\bar{K}'$ starts at a value of skeleton stiffness of $\beta_1^*/R^* = 3.654$; and the loss tangent η starts at a value of zero. This shows that at very low frequency range, the system's behavior is dominated by the stiffness of the solid skeleton. As frequency increases both $\bar{K}'$ and η increase as well. When the loss tangent is maximum ($\omega = \omega_c$), the rate of increase of $\bar{K}'$ is also greatest. At higher frequencies, since relative motion of fluid and solid decreases, the loss tangent becomes small and $\bar{K}'$ tends to a high but constant value. The final value of the storage modulus obtained from Wijesinghe and Kingsbury's quasi-static investigation is

$$\frac{\beta_1^*}{R^*}\left(1+\frac{Q^*+R^*}{\beta_1^*}\right) = 7.17,$$

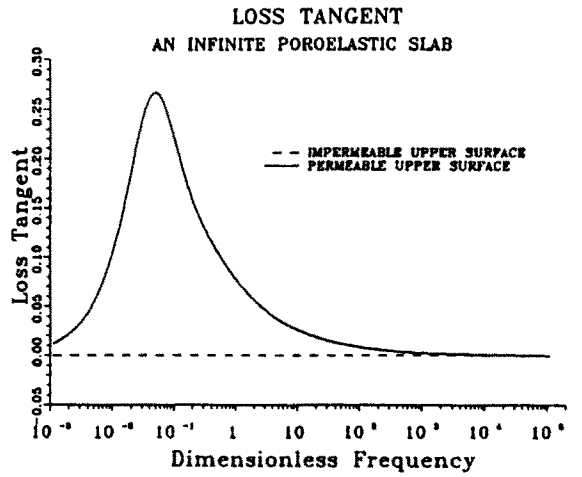

Fig. 2. The loss tangent of an infinite poroelastic slab.

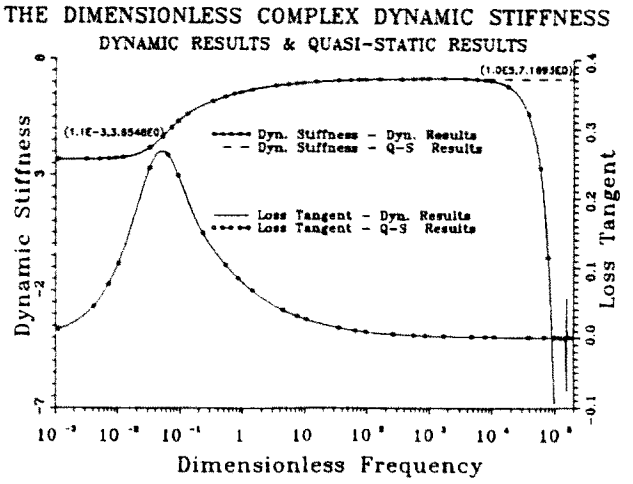

Fig. 3. The dimensionless complex dynamic stiffness—dynamic results and quasi-static results.

which is very close to that predicted by the complete theory. For example, at $\omega^* = 1800$, the value of $\bar{K}'$ obtained from the present study is 7.154. The results of the two analyses start to diverge significantly at $\omega^* = 10^4$, and above this frequency, the resonant response of the dynamic stiffness is predicted only by the complete theory.

DYNAMIC RESULTS AND REDUCED DYNAMIC RESULTS

In the higher frequency range, the resonance phenomena in poroelastic materials observed by Wijesinghe and Kingsbury in their "dynamic" (reduced dynamic) case can be obtained directly from the complete theory results by setting the dissipation coefficient b equal to zero. Figure 4 compares the results for the complete dynamic theory with the results for the reduced dynamic case which excluded the dissipation terms. It is observed that the complete theory predicts a higher fundamental resonant frequency as well as a higher stiffness than that of the reduced dynamic case. For this particular case, the resonant frequency predicted by the complete theory is near the fourth resonance of the reduced theory.

It may be concluded that lack of dissipation terms in the equation results in inaccurate prediction of all resonant frequencies including the lowest.

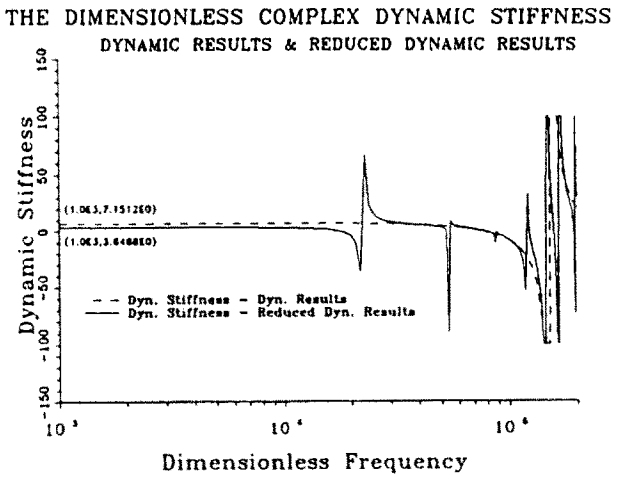

Fig. 4. The dimensionless complex dynamic stiffness—dynamic results and reduced dynamic results.

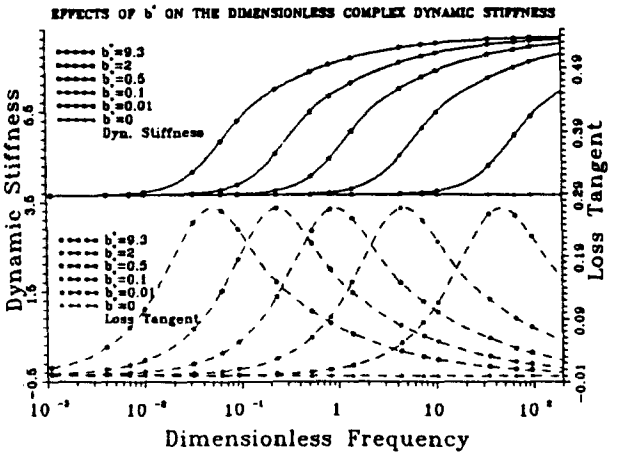

Fig. 5. Effects of dissipation coefficient b^* on the dimensionless complex dynamic stiffness.

EFFECTS OF b^* AND ρ_{12}^* ON A DIMENSIONLESS COMPLEX DYNAMIC STIFFNESS FUNCTION

The influences of the dimensionless coupling apparent mass, ρ_{12}^*, and of the dimensionless dissipation, b^*, on a dimensionless complex dynamic stiffness function are next examined for the case of a slab with a permeable upper surface.

Figure 5 shows results for the influence of b^* on $\bar{K}(i\omega^*)$. It is observed that the critical frequency, ω_c^*, increases as the dissipation, b^*, decreases. When the dissipation term is neglected ($b^* = 0$), the viscous interactions between the fluid and the solid disappear as well. The loss tangent then approaches zero, and the dynamic stiffness of the poroelastic material depends solely on the stiffness of the skeleton (β_1^*/R^*).

For non-zero values of b^*, the value of ω_c decreases as b^* increases, but the maximum value of the loss tangent is essentially independent of b^*. This is in agreement with the findings of Okuno and Kingsbury (1989) who showed that the maximum value of it depends only on the compressibilities of the poroelastic material constituents.

Finally, the influence of the coupling density, ρ_{12}^*, on the amplitude of the maximum dynamic stiffness, $\bar{K}'_{max}$, and the amplitude of the maximum loss tangent, η_{max}, is explored in Fig. 6. When the absolute value of ρ_{12}^* increases from 0 to 1.1336×10^{-9} (ρ_{22}^*), then to 3.7185×10^{-9} (ρ_{11}^*), the amplitudes of $\bar{K}'_{max}$ and η_{max} increase accordingly.

These effects are very small in the low frequency region as shown in the lower part of Fig. 6. As the frequency approaches the layer resonant frequency, however, it is seen that the value of ρ_{12} has a very pronounced effect on the dynamic stiffness. This implies that the as yet unresolved problem of evaluating ρ_{12} must be attacked if Biot's equations are to be used to predict resonant response.

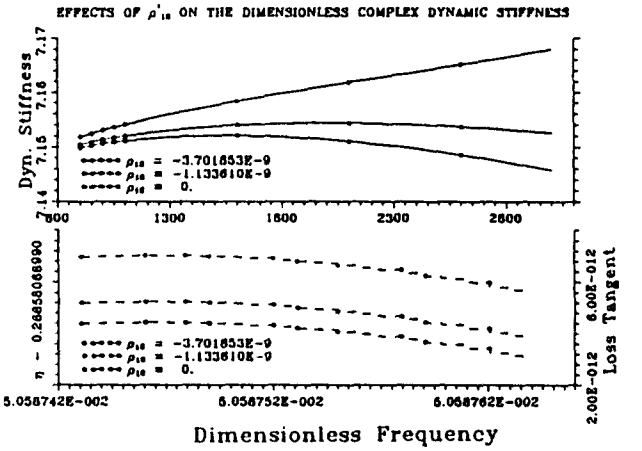

Fig. 6. Effects of ρ_{12}^* on the dimensionless complex dynamic stiffness.

CONCLUSIONS

The complex dynamic stiffness of a poroelastic layer has been determined by solving Biot's complete equations of poroelasticity for the case of an impulsive pressure applied to a surface. The resulting expression is used to study the effects of neglecting either inertia or dissipation terms in the complete theory as well as the effects of surface permeability, dissipation coefficient and coupling density on layer dynamic stiffness and energy dissipation.

It was found that the quasi static theory accurately predicts layer response below the first structural resonant frequency while the reduced dynamic theory does not accurately predict the layer resonant frequencies.

If both surfaces are impermeable, the layer behaves as a homogeneous solid with constant stiffness and zero damping below the resonant frequency. If, on the other hand, flow through a surface is permitted, there is a frequency range in which the storage constant increases and the loss tangent achieves a maximum value.

The frequency of the maximum value of the loss tangent is dependent upon the value of the dissipation coefficient but the maximum value itself is independent of b.

Finally, it is shown that although the coupling density coefficient, ρ_{12}, has little effect on the dynamic stiffness at low frequencies its value must be chosen correctly in order to accurately predict layer response at frequencies approaching the layer resonant frequency.

REFERENCES

Biot, M. A. (1941). General theory of three dimensional consolidation. *J. Appl. Phys.* **12**, 155–164.

Biot, M. A. (1955). Theory of elasticity and consolidation for a porous anisotropic solid. *J. Appl. Phys.* **26**, 182–185.

Biot, M. A. (1956a). General solutions of the equations of elasticity and consolidation for a porous material. *J. Appl. Mech. (Trans. ASME)* **23**, 91–96.

Biot, M. A. (1956b). Theory of propagation of elastic waves in a fluid-saturated porous solid – i: low-frequency range – ii, higher frequency range. *J. Acoust. Soc. Am.* **28**(2), 168–191.

Biot, M. A. and Willis, D. G. (1957). The elastic coefficients of the theory of consolidation. *J. Appl. Mech. (Trans. ASME)* **24**, 594–601.

Chakravarti, N. B. (1962). Dynamic stresses in a poroelastic infinite medium with a spherical cavity. *J.S.E.R.* 309–318.

Garg, S. K., Nayfa, A. H. and Good, A. J. (1974). Compressional waves in fluid-saturated elastic porous media. *J. Appl. Phys.* **45**(5), 1968–1974.

Hong, S. J., Sandhu, R. S. and Wolfe, W. E. (1988). On Garg's solution of Biot's equation for wave propagation in a one-dimensional fluid-saturated elastic porous solid. *Int. J. Num. Anal. Meth. Geomech.* **12**, 627–637.

Kingsbury, H. B. (1984). Determination of material parameters of poroelastic media. In *Fundamentals of Transport Phenomena in Porous Media* (Edited by J. Bear and M. Corapcioglu), pp. 581–615. Martinus Nijhoff, Dordrecht.

Okuno, A. and Kingsbury, H. B. (1989). Dynamic modulus of poroelastic materials. *J. Appl. Mech.* **56**, 535–540.

Wijesinghe, A. M. and Kingsbury, H. B. (1979). On the dynamic behavior of poroelastic materials. *J. Acoust. Soc. Am.* **65**(1), 90–95.